

# Velocity Distributions and Normal Stresses in Viscoelastic Turbulent Pipe Flow

GIANNI ASTARITA and LUIGI NICODEMO

Istituto di Chimica Industriale, University of Naples, Naples, Italy

Pitot tube readings in a viscoelastic turbulent stream are discussed theoretically, and are shown to be made up by a first normal stress contribution, an integral normal stress contribution, and a kinetic contribution. These three contributions are of comparable orders of magnitude. The integral of a Pitot tube scanning curve is shown to yield a momentum average factor of direct physical relevance. Experimental data show that the normal stress contributions are not negligible even in the central region of the pipe, although turbulent flow conditions were reached. Observed values of the relevant parameters are discussed.

Anomalous turbulent behavior of dispersed systems such as fiber suspension has repeatedly been reported. The most striking feature of these phenomena is the drag reduction effect which is observed during turbulent flow of very dilute solutions of some macromolecular substances (1, 10). Although such solutions are to be considered as dispersed systems on the microscopic scale, their macroscopic behavior can be discussed in terms of continuum mechanics, provided a sufficiently generalized rheological behavior is accounted for.

Investigation of the drag reduction effect (1) has led to an interest in the distribution of velocities during turbulent flow of such solutions (1, 12). This paper reports the results of a Pitot tube investigation of the turbulent flow of viscoelastic liquids through circular pipes. Pitot tube readings, as shown below, yield apparent velocities which, in the case of viscoelastic liquids, may be markedly different from the true velocities. Nonetheless, the results of a Pitot tube experiment have direct physical relevance, and they may allow, if independent measurements of true velocities become available, the gain of a quantitative knowledge of the normal stress pattern during turbulent flow of viscoelastic liquids.

## THEORY

Consider a Pitot tube immersed into a stream of an incompressible liquid, flowing at steady state conditions through a circular pipe, and suppose that the Pitot opening lies in the  $r\theta$  plane normal to the flow direction  $x$ . The following hypotheses are made: (1) the Pitot tip has no area; (2) the flow is not altered by the presence of the Pitot; and (3) the Pitot tube is a time integrator.

It has been pointed out recently (9) that viscoelastic liquids may build up a solidlike structure on the Pitot tip, due to the sudden deceleration of flow in this region. Although major elastic effects are indeed to be foreseen at the Pitot tip, it is doubted that a stagnant pocket of liquid may be solidlike, because it is known that Newtonian behavior is approached in stagnant regions. Thus, even if hypothesis (2) is inficiated, the structure which may form on a Pitot tip cannot presumably sustain any pressure difference, so that the actual local impact pressure is transmitted to the Pitot.

Under such assumptions, the pressure reading at the Pitot tube  $p_p$  is given by:

$$p_p = -\bar{\sigma}_x + \frac{\rho \bar{u}_x^2}{2} \quad (1)$$

where  $\bar{\sigma}_x$  is the time-average value of the normal stress in the flow direction. Both  $\bar{\sigma}_x$  and  $\bar{u}_x^2$  are, of course, functions of the Pitot tube position, say of the distance  $r$  from the tube axis.

The pressure  $p_R$  which may be observed at a pressure tap mounted flush to the tube wall at the same axial position is given by

$$p_R = -(\sigma_r)_{r=R} = -(\bar{\sigma}_r)_{r=R} \quad (2)$$

where the instantaneous and the time-average values coincide because any fluctuation is eliminated at the tube wall.

A differential momentum balance in the  $r$  direction reads

$$r(d\bar{\sigma}_r/dr) = \bar{\sigma}_\theta - \bar{\sigma}_r = \bar{\sigma}_\theta^* - \bar{\sigma}_r^* \quad (3)$$

which, upon integration, yields

$$\bar{\sigma}_r = -p_R + \int_r^R (\bar{\sigma}_r^* - \bar{\sigma}_\theta^*) d \ln r \quad (4)$$

The differential Pitot pressure reading thus is given by

$$\begin{aligned} (\Delta p)_p &= p_p - p_R + \\ &= -(\bar{\sigma}_x^* - \bar{\sigma}_r^*) - \int_r^R (\bar{\sigma}_r^* - \bar{\sigma}_\theta^*) d \ln r + \rho \bar{u}_x^2/2 \end{aligned} \quad (5)$$

Equation (5) shows that  $(\Delta p)_p$  is made up of three parts: a first normal stress contribution; an integral normal stress contribution; and a kinetic contribution. When it is assumed that all the deviatoric normal stresses are zero, Equation (5) reduces to the usual interpretation of the differential Pitot pressure.

## Laminar Flow

When the liquid is in laminar flow, time-average and instantaneous values coincide, and Equation (5) reduces to the equation given originally by Savins (12). Savins proposed the use of Equation (5), together with an independent evaluation of the velocity distribution, as a means for measuring the first normal stress difference  $\sigma_x^* - \sigma_r^*$ . In order to make this possible, he assumed that the second normal stress difference  $\sigma_r^* - \sigma_\theta^*$  is zero.

Some comments concerning this assumption seem in order. Although it is by now accepted that the so-called "Weissenberg hypothesis," namely  $\sigma_r^* = \sigma_\theta^*$ , has no a priori justification, experimental evidence (8, 12) indicates that the second normal stress difference is indeed minor as compared to the first one. This does not, however, permit the integral normal stress contribution to be dropped

Gianni Astarita is at the University of Delaware, Newark, Delaware.

from Equation (5), even under laminar flow conditions. In fact, at the tube axis, the first normal stress difference is zero because of symmetry, while the integral contribution is finite. Thus, dropping the integral contribution is admissible only if it is negligible as compared to the kinetic contribution, the latter again having its maximum value at the tube axis.

An evaluation of the relative importance of the various terms in Equation (5) under laminar flow conditions can be obtained by assuming a power law model for both the tangential and the normal component of stress:

$$\tau_{xr} = b |du/dr|^{n-1} (-du/dr) \quad (6)$$

$$\sigma_x^* - \sigma_r^* = a |du/dr|^{s-2} (-du/dr)^2 \quad (7)$$

$$\sigma_r^* - \sigma_\theta^* = \beta (\sigma_x^* - \sigma_r^*) \quad (8)$$

When Equations (6) to (8), together with the tangential momentum-balance equation

$$\tau_{xr}/\tau_o = r/R \quad (9)$$

are used, the following expressions for the radial distributions of velocity and of normal stress differences are obtained:

$$\sigma_x^* - \sigma_r^* = a \left( \frac{\tau_o}{b} \right)^{s/n} \left( \frac{r}{R} \right)^{s/n} \quad (10)$$

$$\int_r^R (\sigma_r^* - \sigma_\theta^*) d \ln r = a \frac{\beta n}{s} \left( \frac{\tau_o}{b} \right)^{s/n} \left[ 1 - \left( \frac{r}{R} \right)^{s/n} \right] \quad (11)$$

$$u_x = \left( \frac{\tau_o}{b} \right)^{1/n} R \frac{n}{n+1} \left[ 1 - \left( \frac{r}{R} \right)^{\frac{n+1}{n}} \right] \quad (12)$$

From Equations (10), (11), and (12), the relative importance of the three contributions to the differential Pitot reading can be evaluated, provided reasonable values are assigned to the rheological parameters  $s$ ,  $n$ ,  $\beta$ , and  $a$ . In order to carry out an order-of-magnitude analysis,  $s$  and  $n$  may be taken to be 2.0 and 1.0, respectively. According to the Weissenberg hypothesis,  $\beta = 0$ ; some data relative to solutions of the same polymer used in this work (9) indicate that a value of 0.2 may be considered reasonable. Values of  $a$  of the order of 1 g./cm. are to be considered reasonable in view of available experimental evidence (8). Thus, at the tube axis, the ratio of the integral normal stress contribution to the kinetic contribution can be evaluated at the order of magnitude of

$$\frac{\int_0^R (\sigma_r^* - \sigma_\theta^*) d \ln r}{(\rho u_x^2/2)_{r=R}} = \frac{\beta a}{s} \frac{2(n+1)^2}{n} \frac{(\tau_o/b)^{\frac{s-2}{n}}}{R^2 \rho} \cong 0.8 \frac{a}{R^2 \rho} \quad (13)$$

Thus, when a liquid with the density of water is flowing through a 2-cm. I.D. tube, the integral normal stress contribution at the tube axis may be as much as 80% of the kinetic contribution, although the second normal stress difference is no more than 20% of the first normal stress difference. At the tube wall, of course, all the contributions except the first normal stress, which has its maximum value at the tube wall, vanish.

Finally, it should be mentioned that, if  $\beta$  indeed has positive values, both normal stress contributions are of a direction opposite to the kinetic contribution.

#### Turbulent Flow: Purely Viscous Liquids

Let an apex (') indicate the fluctuating component of any quantity, and let  $\mu$  be the shear-dependent viscosity

of the liquid. The time-average deviatoric normal stresses are given by

$$\overline{\sigma_i^*} = -\rho \overline{u_i'^2} + 2\mu \overline{\frac{\partial u_i}{\partial x_i}} \quad (14)$$

where  $\partial u_i/\partial x_i$  is the covariant derivative of the velocity in the  $i$  direction to the  $i$  coordinate.

For Newtonian fluids,  $\mu$  is constant and

$$\mu \overline{\frac{\partial u_i}{\partial x_i}} = \mu \frac{\partial \overline{u_i}}{\partial x_i} = 0 \quad (15)$$

so that the only deviatoric normal stress is a Reynolds stress,  $\rho \overline{u_i'^2}$ . This is known to be an intrinsic source of error in Pitot tube readings of mean velocities (6). Nonetheless, the Reynolds stresses are known to be negligible in Newtonian fluids when compared to the kinetic contribution; even at the outer limit of the buffer layer, the Reynolds stress amounts to no more than 1% of the kinetic contribution (6, 7, 14). Notice that if the turbulence were isotropic, the diagonal elements of the Reynolds stress tensor would be all equal, so that the deviatoric normal Reynolds stresses would be zero. In turbulent pipe flow, the turbulence is not isotropic, so that in principle a Reynolds stress correction of the integral type should be considered for Pitot tube readings.

Even in purely viscous non-Newtonian fluids, Equation (15) breaks down, because the viscosity is not constant. Nonetheless, the effect should be minor, as shown below.

For incompressible fluids, the viscosity is a function of the second and third invariants of the rate-of-strain tensor (Reiner-Rivlin fluids are not considered here), but it will be assumed as usual that it depends only on the second invariant.

The only nonvanishing component of the time-average component of the rate-of-strain tensor is the  $rx$  component which will be indicated as  $\Gamma$ . Thus, the second invariant is given by

$$\begin{aligned} \Delta:\Delta &= \Delta':\Delta' + \Gamma^2 + 2\Gamma \left( \frac{\partial u'_x}{\partial r} + \frac{\partial u'_r}{\partial x} \right) = \\ &= \overline{\Delta:\Delta} + 2\Gamma \left( \frac{\partial \overline{u'_x}}{\partial r} + \frac{\partial \overline{u'_r}}{\partial x} \right) \quad (16) \end{aligned}$$

Equation (16) is interesting in two respects. First, it shows that the fluctuating component of  $\Delta:\Delta$  is, with possibly the exception of the centerline region, minor as compared to the time-average component; thus, the effective viscosity is approximately constant. Second, Equation (16) shows that the time-average value of  $\Delta:\Delta$  is not equal to  $\overline{\Delta:\Delta}$ ; thus, the effective viscosity is not equal to what would be calculated from the local value of the time-average shear rate.

If the viscosity is approximately constant, Equation (15) is still approximately valid, so that a Pitot tube reading, for purely viscous liquids, may still be regarded as a kinetic pressure reading (3). Indeed, Pitot tube determinations of velocity distributions in purely viscous liquids have given satisfying results, with no apparent inconsistencies (3 to 5).

#### Turbulent Flow: Viscoelastic Liquids

When turbulent flow of viscoelastic liquids is considered, none of the simplifications made in treating the purely viscous case can be retained. Even if hypothesis (2) is still accepted, the local values of the deviatoric normal stresses are not zero for two reasons: because even the time-average velocity distribution gives rise to non-zero values of the deviatoric normal stresses (as in the

case of laminar flow), and because the essential nonlinearity of the constitutive equation of viscoelastic liquids basically destroys the possibility of admitting the validity of even a vague analog of Equation (15). This, of course, means that the values of  $\bar{\sigma}_x^*$  are not, in turbulent flow, related to the time-average velocity distributions in the same way as they are in the laminar flow case.

Let  $v_x$  be the *apparent velocity*, defined as

$$v_x = \epsilon \sqrt{2 |(\Delta p)_p| / \rho} \quad (17)$$

where  $\epsilon$  is a quantity whose numerical value is unity, and whose sign is the same as that of  $(\Delta p)_p$ . Introduction of this quantity is required to obtain the usual interpretation of a negative pressure difference as an indication of a reverse flow condition.

Insofar as the two normal stress contributions in Equation (5) are both negative, it is expected that  $v_x$  is smaller than  $\bar{u}_x$  everywhere. Moreover, negative values of  $v_x$  are not to be excluded in the proximity of the wall, where the first normal stress difference may be important, while the kinetic contribution is small.

The overall relative importance of the two normal stress contributions in Equation (5) may be appreciated by evaluating the ratio  $q$  of the apparent to the true flow rate (the latter is easily measured independently):

$$q = \frac{\int_0^R 2\pi r v_x dr}{\pi R^2 U} = \int_0^1 \frac{v_x}{U} d\left(\frac{r^2}{R^2}\right) \quad (18)$$

Thus, a Pitot tube scanning over a diameter allows the importance of the normal stresses in turbulent flow to be evaluated, which would manifest through an apparent noncheck of the overall mass balance. Of course, a minor normal stress effect would be masked if the true flow rate is not measured with great care.

A more important result can be obtained from a Pitot tube scanning experiment. In fact, consider that in classical fluid mechanics problems, when a momentum balance among two different sections is made, the momentum flux at any section is usually written as

$$M = p + \alpha \frac{\rho U^2}{2} \quad (19)$$

where  $p$  is the static pressure and  $\alpha$  is a momentum-average factor, defined by

$$\alpha = \int_0^1 \frac{\bar{u}_x^2}{U^2} d\left(\frac{r^2}{R^2}\right) \quad (20)$$

In practice,  $p$  would be taken as the pressure which can be measured at a tap mounted flush to the tube wall. It might thus be useful to apply Equation (19) also to viscoelastic liquids, in the form

$$M = p_R + \alpha \frac{\rho U^2}{2} \quad (21)$$

where, of course,  $\alpha$  is *not* given by Equation (20).

The momentum flux in the viscoelastic case is given by

$$M = \int_0^1 \left( -\bar{\sigma}_x + \frac{\rho \bar{u}_x^2}{2} \right) d\left(\frac{r^2}{R^2}\right) \quad (22)$$

Equation (22) reduces to Equation (21) if the Reynolds stress contribution is neglected as usual, and if  $\alpha$  is defined as

$$\alpha = \int_0^1 \frac{v_x^2}{U^2} d\left(\frac{r^2}{R^2}\right) \quad (23)$$

say, if the Pitot tube readings are interpreted conventionally, and apparent velocities are substituted for true

velocities in Equation (20). Of course, there is no reason to expect that  $\alpha$  values are larger than unity, in contrast with the purely viscous case. Other parameters characterizing the elastic contribution to the Pitot reading could be imagined, but  $\alpha$  seems to be the most directly meaningful, and it can be used in an overall balance equation such as (21).

## EXPERIMENTAL

The loop used for the experiments consisted of feed tank, centrifugal pump, flow rate control valve, flow meter, temperature reading, test section, and discharge tube. Opposing requirements had to be met with compromise solutions. Due to the high flow rates required and to the long time for each run (approximately 4 hr.), a once through experiment would have required a prohibitively large batch of solution, so that recirculation was unavoidable. Recirculation causes a progressive change of the rheological properties, which was observed as a slowly decreasing pressure drop. All the runs for which the percentage fall of the pressure drop at the end of the run was more than 5% of the value at the beginning were discarded. Samples of the liquid were taken approximately halfway in the run and used for determining rheological properties.

The test section consisted of a 130 cm. long, 0.96 cm. I.D. Lucite tubing. Two pressure taps were mounted flush to the tube wall at a relative distance of 10 cm. close to the outlet section. A 0.05 cm. I.D., 0.08 cm. O.D. Pitot tube could be made to scan a horizontal diameter at the same section where the second pressure tap was mounted. The Pitot tube was bent upward, so that only the part lying in the direction of flow was located in the plan of scanning (preliminary runs made with the Pitot bent in the plane of scanning yielded results which were not symmetrical with respect to the tube axis).

A fresh solution was prepared for each run. In order to obtain reproducible rheological properties, all the solutions were prepared by dilution of a single large batch of concentrated solution. The solutions used were aqueous solutions of ET597 manufactured by Dow Chemical Company. Rheological data for these solutions are reported elsewhere (2).

For each run, the pressure drop, that is, the difference  $\Delta p_R$  among the readings at the two wall pressure taps, was recorded, as well as the Pitot tube differential readings and the corresponding radial positions of the Pitot tube. A complete scanning was made on half a diameter, while a few readings were taken at symmetrically opposite positions in order to check the symmetry. Original data are recorded.

An Ostwald-Fenske viscometer and a standard capillary viscometer were used to determine the shear stress-shear rate curve in viscometric flow. The solutions used are known to be markedly elastic, and elastic properties have been measured (2). Rheological data are recorded.

## RESULTS

### Preliminary Data

In order to check the reliability of the experimental setup, preliminary runs were made with water (under turbulent flow conditions), and with an aqueous solution of sugar with a kinematic viscosity of 0.155 sq. cm./sec. (under laminar flow conditions). The pressure drops agreed within 4% with the values calculated for turbulent flow through smooth tubes and from the Poiseuille equation, respectively. The velocity distributions were also in good agreement with accepted correlations, as some typical data reported in Figure 1 show. In this figure, observed values of  $v_x/U$  are compared with the theoretical line for laminar flow and with the accepted turbulent flow velocity distribution (14):

$$\bar{u}_x/U = 1.20 \left( 1 - \frac{r}{R} \right)^{1/7} \quad (24)$$

The data in Figure 1 are plotted in the form suggested by Equation (18) for an immediate mass balance check;

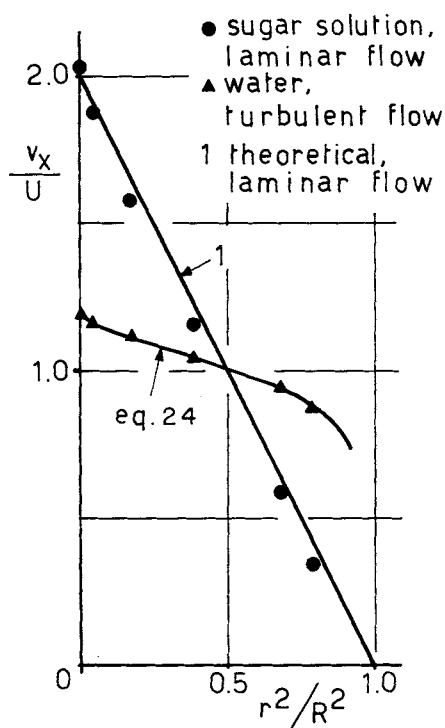


Fig. 1. Velocity distributions in Newtonian liquids.

for all the runs with Newtonian liquids,  $q$  values between 0.96 and 1.03 were observed. Thus, the maximum error in the flow rate measuring system is appreciated at no more than 4%.

#### Runs with Viscoelastic Liquids: Friction Velocities

Eleven runs were chosen for detailed analysis, after discarding a number of previous runs because of minor experimental shortcomings. A summary of results is reported in Table 1.

For each run the wall tangential stress  $\tau_o$  and the friction velocity  $u_f$  were calculated from the measured  $\Delta p_R$  value through the equation

$$u_f = \sqrt{\tau_o/\rho} = \sqrt{\Delta p_R R/2 L \rho} \quad (25)$$

where  $L$  is the distance among the two pressure taps.

Observed values of  $u_f$  are plotted in Figure 2 vs. the average velocity  $U$ . Such a plot is preferable to a  $\lambda$  vs.  $N_{Re}$  plot where drag reduction effects are to be discussed. The line calculated from Blasius' equation

$$u_f = \sqrt{\frac{\lambda}{8}} U = 0.199 N_{Re}^{-1/8} U \quad (26)$$

for water is reported for comparison. While the water data lie almost exactly on this line, the viscoelastic liquid data clearly show the well-known drag reduction effect. Of course,  $u_f$  values relative to different liquids cannot be compared directly, but, as shown for example by Equation (26), a Reynolds number correction is needed. But, in the case of the aqueous solutions considered here, which, obviously under no conditions display apparent viscosities lower than that of water,  $u_f$  values lower than the values observed with water at the same flow rate can only be attributed to a drag reduction effect.

#### Apparent Velocity Distributions

For each run, the Pitot tube readings over a diameter were elaborated to calculate the apparent velocities  $v_x$  according to Equation (17). Plots of  $v_x/U$  vs.  $(r/R)^2$ , such as reported in Figure 3 for runs C and M, have been made for each run and values of  $q$  have been calculated, as reported in Table 1. In calculating the values of  $q$ , the velocity distribution was extrapolated to the tube wall with the arbitrarily chosen rule of connecting the last

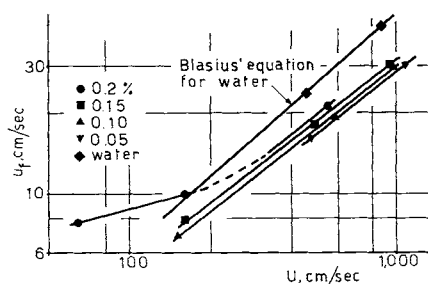


Fig. 2. Friction velocity data.

TABLE 1. SUMMARY OF RESULTS

Run	Concentration, % by weight	$U$ , cm./sec.	$u_f$ , cm./sec.	$q$	$\alpha$	$N_{Re}$	$(v_x/U)_{r=0}$
A	0.05	475	16.1	0.864	0.81	27,400	1.09
B	0.05	1,080	30.4	0.850	0.82	62,300	1.14
C	0.10	151	7.03	0.707	0.63	5,870	1.27
D	0.10	591	18.5	0.763	0.65	36,000	1.12
E	0.10	985	29.6	0.742	0.60	60,000	1.12
F	0.15	162	8.48	0.885	0.96	4,250	1.40
G	0.15	500	17.7	0.790	0.84	18,450	1.24
H	0.15	952	29.8	0.807	0.76	41,900	1.19
I	0.20	63	7.81	1.00	1.30	885	1.65
L	0.20	162	9.80	0.850	1.03	3,060	1.49
M	0.20	550	21.2	0.918	0.96	9,600	1.26
Laminar flow, Newtonians:				1.000	4/3		2.00
Turbulent flow, Newtonians:				1.000	1.02		1.20
14*	0.2 Carbopol	447	22.7	1.034	1.06	28,500	1.23
13*	0.2 Carbopol	1,385	60.6	1.004	1.02	107,550	1.22
33*	0.4 Carbopol	463	26.0	0.980	1.06	6,100	1.27
9*	0.4 Carbopol	1,360	63.8	0.987	0.98	23,240	1.20
20*	14.0 Clay	789	36.6	0.992	1.04	12,900	1.23
17*	14.0 Clay	950	42.0	0.965	0.94	17,150	1.22

\* Bogue's data.

point, taken at  $r = 0.43$  cm., that is, at  $(r/R)^2 = 0.79$ , with the point  $v_x = 0$ ,  $r = R$ , by means of a straight line. In view of the fact that apparent velocities are probably negative in the immediate neighborhood of the wall, this procedure presumably leads to an overestimation of the value of  $q$ .

With the exception of run *I* (which will be discussed below), all the values of  $q$  observed are markedly lower than unity by an amount which cannot be attributed to faulty flow rate determinations. In the case of run *C* the apparent flow rate is as much as 30% lower than the true flow rate. This implies that elastic effects are very important, and that  $v_x$  values should by no means be considered as true local velocities.

The values of  $q$  reported in Table 1 seem to pass through a minimum at a concentration of 0.1%; this statement is based on a comparison made at equal volumetric flow rate. The state-of-the-art understanding of the drag reduction phenomenon does not indicate if values of  $q$  should be compared at equal flow rate, or at equal Reynolds number, or at equal fractional drag reduction. Nonetheless, the pressure drop is known to undergo a minimum if values at different concentrations are compared at equal flow rate, and the minimum of  $q$  may somehow be related to this.

Apparent velocity defects have been calculated for each run as

$$v_d = \frac{(v_x)_{r=0} - v_x}{u_f} \quad (30)$$

and have been plotted as usual vs. the log of  $(R-r)/R$ . The plots for runs *C* and *M* are reported in Figure 4.

It is interesting to observe that plots such as in Figure 4 had much the same behavior as those reported by Shaver and Merrill (13), in contrast with the results relative to purely viscous liquids of Eissenberg and Bogue (5), which practically coincide with the Newtonian results. Shaver and Merrill were apparently unaware of the elastic character of the liquids they used, and have interpreted their values of  $v_x$  as being true velocities. Thus,

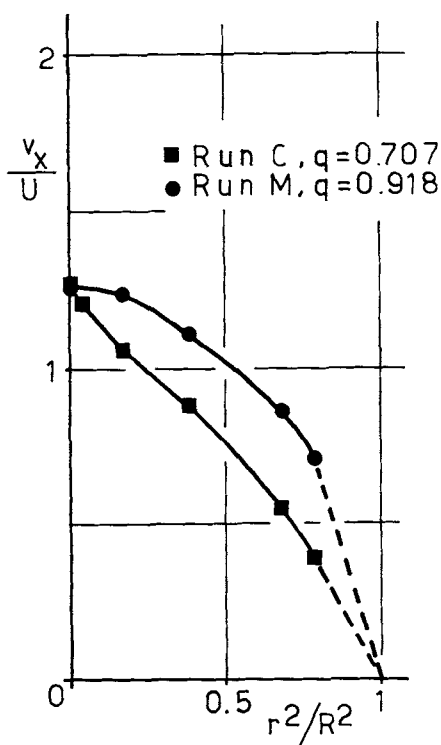


Fig. 3. Plot for evaluation of  $q$ .

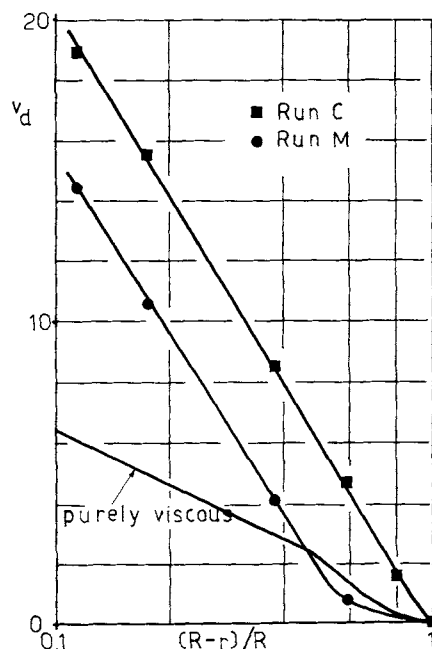


Fig. 4. Apparent velocity defect plot.

from plots such as in Figure 4, they conclude that velocity profiles are less blunt than in Newtonian liquids or, for that matter, in purely viscous liquids which are known to display Newtonian velocity profiles in turbulent flow, as shown by Bogue and Metzner (4). This conclusion, although possibly true for liquids which display drag reduction effects (1), should be considered in view of the present results as not being substantiated by experimental evidence.

Shaver and Merrill claim that their mass balances did check, say, in the present terminology, that their observed values of  $q$  did not appreciably differ from unity. In view of the present results, this claim is somewhat surprising. Shaver and Merrill state that they have ascertained the absence of any significant slip at the wall (actually, negative values of  $v_x$  are expected at the tube wall) because their overall mass balances did check. This we could not understand, because, assuming that true velocities are measured, the overall mass balance would check even in the presence of wall slip.

#### Values of $\alpha$

For each run, a plot was made of  $(v_x/U)^2$  vs.  $(r/R)^2$ . The area under a curve in such a plot equals, according to Equation (23), the value of the momentum-average factor  $\alpha$ . Observed values are reported in Table 1.

In the same table values of the Reynolds number for each run are also reported. These have been calculated by means of the accepted procedure for non-Newtonian fluids (see for example reference 10). Values of the apparent flow index have been obtained with standard capillary viscometric techniques in the shear stress range prevailing at the tube wall in the actual run, and range between 0.7 for the 0.2% solution and almost 1.0 for the 0.05% solution.

Values of  $\alpha$  are plotted vs. the Reynolds number in Figure 5. With the exception of one point, all the data seem to lie on a single curve, which does not show the abrupt transition from laminar to turbulent flow conditions which is typical of purely viscous liquids. In the same figure, the curve relative to purely viscous liquids is also reported; in the laminar flow region, the position of the purely viscous line is a weak function of the apparent flow index.

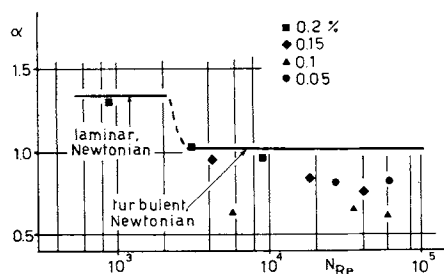


Fig. 5. Values of  $\alpha$  in viscoelastic liquids.

Both the effects observed, namely,  $q$  and  $\alpha$  values systematically lower than unity, are to be attributed to the elastic character of the liquids used. In fact, simple non-Newtonianism of purely viscous fluids would not cause these effects, as discussed previously, and as clearly shown by Bogue's data (3), relative to presumably purely viscous fluids such as Carbopol solutions and clay suspensions. From Bogue's original velocity profiles, values of  $q$  and  $\alpha$  have been calculated and some of these are included in Table 1 for comparison. It is apparent that in the case of Bogue's data, neither the  $q$  nor the  $\alpha$  value is significantly different from the predicted Newtonian values of 1.0 and 1.02, respectively.

In contrast with this, the  $\alpha$  values relative to viscoelastic liquids are in the turbulent flow region consistently lower than unity, which indicates that the pull in the direction of flow due to elastic effects is not negligible as compared to the kinetic momentum flux.

For the 0.2% solution, run I corresponds to strictly laminar flow conditions and run L is probably in the transition region. The laminar flow run I is the only one for which a  $q$  value of unity has been observed. This seems to indicate that normal stress effects are in this case negligible. As a matter of fact, at the estimated wall shear rate of 600  $\text{sec}^{-1}$ , the first normal stress difference can be evaluated from rheological data at 100 dynes/sq. cm. This is of course the highest value so that the overall effect over the cross section can be estimated at no more than 50 dynes/sq. cm. When this is compared with a kinetic momentum flux of 4,000 dynes/sq. cm. it is not surprising that the overall effect does not manifest with a nonunity value of  $q$ . Correspondingly, the value of  $\alpha$  is 1.30, which corresponds to the laminar flow value for a power law liquid with a flow behavior index of 0.75.

This should be compared with the fact that in turbulent flow conditions, the normal stress effect is conspicuous, as shown by abnormally low values of both  $q$  and  $\alpha$ , even when the first normal stress difference corresponding to the wall shear rate is negligible as compared to the kinetic momentum flux. This means that elastic effects in the central region of the tube are much larger than at the wall, in contrast with the laminar flow case. This is not surprising in view of the inherently unsteady (in the Lagrangian sense) nature of turbulent flow, which may well trigger important elastic effects in fluids which possess a memory. Drag reduction is a macroscopically conspicuous manifestation of such major elastic effects.

## CONCLUSIONS

We are aware of the fact that, in the case of viscoelastic liquids, some doubt exists on whether a Pitot tube measurement yields at all the local impact pressure, even including normal stresses. Also, we know that Pitot tube results are open to discussion as long as no independent measurement of true local velocities is available.

Nonetheless, if hypothesis (2) is accepted, the results of Pitot tube scanning experiments yield one physically

meaningful quantity, namely, the value of  $\alpha$ . The results of the present work show that in turbulent flow unexpectedly low values are obtained.

## ACKNOWLEDGMENT

Domenico Acierio should be credited for most of the experimental work.

## NOTATION

- $a$  = rheological parameter defined by Equation (7),  $\text{g./}(\text{cm.})(\text{sec.}^{2-s})$
- $b$  = rheological parameter defined by Equation (6),  $\text{g./}(\text{cm.})(\text{sec.}^{2-s})$
- $L$  = distance among pressure taps, cm.
- $M$  = momentum flux,  $\text{g./}(\text{cm.})(\text{sec.}^2)$
- $n$  = exponent in Equation (6), dimensionless
- $p$  = static pressure,  $\text{g./}(\text{cm.})(\text{sec.}^2)$
- $p_p$  = pressure reading at Pitot tube,  $\text{g./}(\text{cm.})(\text{sec.}^2)$
- $p_R$  = pressure reading at wall tap,  $\text{g./}(\text{cm.})(\text{sec.}^2)$
- $(\Delta p)_p$  = differential Pitot reading,  $\text{g./}(\text{cm.})(\text{sec.}^2)$
- $(\Delta p)_R$  = pressure drop,  $\text{g./}(\text{cm.})(\text{sec.}^2)$
- $q$  = ratio of apparent to true flow rate, dimensionless
- $r$  = distance from tube axis, cm.
- $R$  = tube radius, cm.
- $s$  = exponent in Equation (7), dimensionless
- $u$  = local velocity, cm./sec.
- $u_f$  = friction velocity, cm./sec.
- $U$  = average velocity, cm./sec.
- $v_x$  = apparent velocity, cm./sec.
- $v_d$  = apparent velocity defect, dimensionless
- $x_i$  = any coordinate direction, cm.
- $N_{Re}$  = Reynolds number, dimensionless,  $= 2 R U \rho / \mu$

## Greek Letters

- $\alpha$  = momentum average factor, dimensionless
- $\beta$  = second-to-first normal stress difference ratio, dimensionless
- $\Gamma$  =  $rx$  component of  $\Delta$ ,  $\text{sec.}^{-1}$
- $\Delta$  = rate-of-strain tensor,  $\text{sec.}^{-1}$
- $\tilde{\epsilon}$  = + 1 when  $(\Delta p)_p > 0$ ; = - 1 when  $(\Delta p)_p < 0$ , dimensionless
- $\lambda$  = friction factor, dimensionless
- $\mu$  = apparent viscosity,  $\text{g./}(\text{cm.})(\text{sec.})$
- $\rho$  = density,  $\text{g./cc.}$
- $\sigma$  = normal stress,  $\text{g./}(\text{cm.})(\text{sec.}^2)$
- $\tau$  = tangential stress,  $\text{g./}(\text{cm.})(\text{sec.}^2)$
- $\tau_o$  = wall value of  $\tau$ ,  $\text{g./}(\text{cm.})(\text{sec.}^2)$

## Superscripts

- $*$  = deviatoric component,  $\sigma_i^* = \sigma_i - 1/3 \sum \sigma_i$
- $'$  = fluctuating component
- $\text{—}$  = time-average component

## Subscripts

- $x, r, \theta$  = axial, radial, tangential components
- $i$  = any one of the three coordinate components

## LITERATURE CITED

1. Astarita, Gianni, *Ind. Eng. Chem. Fundamentals*, **4**, 354 (1965).
2. ———, and Luigi Nicodemo, *ibid.*, in press.
3. Bogue, D. C., Ph.D. thesis, Univ. Delaware, Newark (1960).
4. ———, and A. B. Metzner, *Ind. Eng. Chem. Fundamentals*, **2**, 143 (1963).
5. Eissenberg, D. M., and D. C. Bogue, *A.I.Ch.E. J.*, **10**, 723 (1964).

6. Hinze, J. O., "Turbulence," McGraw-Hill, New York (1959).
7. Levich, V. G., *Acta Physicochim. U.R.S.S.*, **19**, 117 (1943).
8. Markowitz, H., and D. B. Brown, "Symp. II Order Effects, Haifa 1962," p. 585, Pergamon, New York (1964).
9. Metzner, A. B., personal communication (June, 1965).
10. ———, and M. G. Park, *J. Fluid Mech.*, **20**, 291 (1964).
11. Oldroyd, J. G., "Symp. II-Order Effects, Haifa 1962," p. 520, Pergamon, New York (1964).
12. Savins, J. C., *A.I.Ch.E. J.*, **11**, 673 (1965).
13. Shaver, R. G., and E. W. Merrill, *ibid.*, **5**, 181 (1959).
14. Schlichting, Hermann, "Grenzschicht-Theorie," Brown (1951).

Manuscript received October 19, 1965; revision received December 13, 1965; paper accepted December 23, 1965.

# Experimental Vapor-Liquid Equilibrium Data for Propane-Isobutane

HOWARD HIPKIN

C. F. Braun and Company, Alhambra, California

Isothermal vapor-liquid equilibrium data for propane-isobutane, a system of industrial importance, have been obtained in two pieces of apparatus at temperatures from 20° to 250°F. Over this temperature range, propane-isobutane form ideal solutions. The paper discusses the sampling errors which occur in volatile systems.

There are several reasons for making an experimental investigation of the propane-isobutane system, besides the fact that it has not been reported previously. This system controls the separation in all depropanizers, columns that have caused more than their share of design and operating troubles. Many depropanizers operate at pressures above 250 lb./sq.in., where the relative volatility is less than 2.0, and where the magnitude of the relative volatility has a great effect on both number of trays and minimum reflux ratio. Both these factors materially affect the cost of the fractionator. This paper presents experimental data for five isotherms from 20° to 250°F., covering most of the two-phase region above atmospheric pressure.

## APPARATUS

The data were taken in two different pieces of apparatus. The 20°F. isotherm was run in the low-temperature unit shown schematically in Figure 1. This type of equilibrium apparatus has been used by Dodge and Dunbar (1), Katz and co-workers (2 to 6), Price and Kobayashi (7), and by Cines et al. (8, 9), among others. Ruhemann (10) has stated that this is the most accurate and reliable of all low-temperature methods.

The apparatus of Figure 1 is entirely of stainless steel, operates from ambient to -300°F. at pressures to 3,000 lb./sq. in. abs., and embodies some interesting design features. The cell has a gauge-glass window to permit observation of solids or a second liquid phase. The bath temperature is automatically controlled to within 0.05°F. Pressures are read on a dead-weight gauge, isolated from the system by a sensitive diaphragm. Temperature in the cell is read with a laboratory platinum resistance thermometer and a Mueller bridge. Vapor is circulated around the loop with a diaphragm compressor to eliminate leakage and oil contamination. There are two liquid sample valves to permit sampling coexisting liquid phases.

The pressure still used for superambient temperatures is based on the design of Jones, Schoenborn, and Colburn (11). Similar stills for atmospheric pressure or vacuum have been

used by Scatchard, Raymond, and Gilman (12), Amick et al. (13), Hipkin and Myers (14), and Weber et al. (15 to 21). In all these devices circulation of the vapor phase is accomplished thermally by condensing the vapor, draining the condensate to a point below the still, revaporizing it, and passing it up through the still liquid.

The apparatus of Figure 2 operates with a refrigerant circulating between the still condenser, where it picks up heat and is partly vaporized, and the head tank, where it surrenders heat to the primary coolant and is condensed. The pressure level in the still is set by the temperature of the refrigerant and by the heat input to the still vaporizer. The temperature of the refrigerant is set, in turn, by the choice of primary coolant (dry ice, water, air, or boiling water) and by the heat input to the head-tank heaters. To operate, a vapor-recirculating still must be kept adiabatic. As in the Hipkin and Myers still (14), this is accomplished by surrounding the body of the still with a vapor jacket, maintained at the same temperature as the still by a differential thermocouple which controls the heat input to the jacket heaters. The jacket condenser is

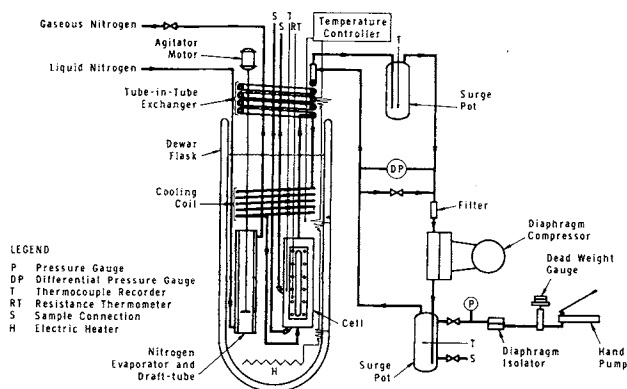


Fig. 1. Low-temperature vapor-liquid equilibrium apparatus.